



*International Journal Of*  
**Recent Scientific  
Research**

ISSN: 0976-3031

Volume: 6(12) December -2015

SYNTHESIS AND CHARACTERIZATION OF NANO TITANIUM DIOXIDE VIA  
SOL GEL PROCESS AT DIFFERENT CALCINATION TIME AND TEMPERATURE

Kavitha V, Ramesh P.S and Geetha D



THE OFFICIAL PUBLICATION OF  
INTERNATIONAL JOURNAL OF RECENT SCIENTIFIC RESEARCH (IJRSR)  
<http://www.recentscientific.com/> [recentscientific@gmail.com](mailto:recentscientific@gmail.com)



**RESEARCH ARTICLE**

**SYNTHESIS AND CHARACTERIZATION OF NANO TITANIUM DIOXIDE VIA SOL GEL PROCESS AT DIFFERENT CALCINATION TIME AND TEMPERATURE**

**Kavitha V<sup>1</sup>, Ramesh P.S<sup>2\*</sup> and Geetha D<sup>3</sup>**

<sup>1</sup>Department of Physics, Periyar University, Salem,-636 011, Tamil Nadu, India

<sup>2</sup>Physics Wing DDE

<sup>3</sup>Department of Physics, Annamalai University, Annamalainagar, - 608 002, Tamil Nadu, India

**ARTICLE INFO**

**Article History:**

Received 15<sup>th</sup> September, 2015

Received in revised form 21<sup>st</sup>

October, 2015

Accepted 06<sup>th</sup> November, 2015

Published online 28<sup>st</sup> December, 2015

**Key words:**

Sol-gel route, calcination time, calcination temperature, Titanium dioxide, spheroidal

**ABSTRACT**

Nano particles of Titanium dioxide are prepared by using a sol-gel route by using hydrolysis of Titanium tetraisopropoxide with ethanol and water mixture as titania source. After heat treatment of the samples, we characterized their structures and basic properties by using conventional XRD, FT-IR, scanning electron microscopy (SEM), UV-Vis spectroscopy and photoluminescence spectroscopy (PL). The X-ray diffraction pattern revealed that the calcined sample of TiO<sub>2</sub> has both anatase and rutile phases. The spherical shape or spheroidal shape was observed using scanning electron microscopy. The rate of recombination and transfer behavior of the photo excited electron-hole pairs in the semiconductors was recorded by photoluminescence. It was found that annealing could improve the crystallization of TiO<sub>2</sub> powders and accelerated the phase transformation from anatase to rutile. The result shows that the different calcination time and calcination temperature, have a lot of influences upon the properties of nano TiO<sub>2</sub>.

**Copyright © Kavitha V, Ramesh P.S and Geetha D., 2015**, this is an open-access article distributed under the terms of the Creative Commons Attribution License, which permits unrestricted use, distribution and reproduction in any medium, provided the original work is properly cited.

**INTRODUCTION**

Titanium is the ninth most abundant element in the Earth's crust [1]. Titanium dioxide (TiO<sub>2</sub>) has high thermal and chemical stability and high transmittance in the visible spectral range [2]. Moreover, it is nontoxic, and applicable for biological coatings, optical devices, and photo electrochemical conversion, environmental photocatalytic processes such as prevention of strains, sterilization and removal of pollutants from air and water, TiO<sub>2</sub> properties are strongly related to phase structure, morphology and particle size distribution. As nanosized particles, these materials exhibit broad band UV absorption, a benefit that currently has been exploited in sunscreen applications. Also, the addition of nanoparticles would likely enhance the stiffness, toughness and service life of polymeric materials [3]. Titanium dioxide is widely known as a material with an excellent photocatalytic activity. There are two main obstacles for the practical application of TiO<sub>2</sub> photocatalyst: low quantum efficiency and restriction to short wavelength excitation. Furthermore, titania possess high available surface areas, which are beneficial for aqueous photocatalytic reactions [4].

Titanium dioxide has three principal crystallographic structures called anatase (tetragonal), rutile (tetragonal) and brookite (orthorhombic). Among these, anatase has excellent chemical and physical properties for environmental purification and is thermodynamically more stable than rutile phase. Numerous methods have been developed for the synthesis of nanostructures such as vapor-liquid-solid [5], chemical vapor deposition (CVD) [6], Laser- assisted catalytic growth [7], electron beam lithography, sol-gel [8], solvothermal [9], and the filling of templates with colloidal oxide particulars [10]. These nanoparticles can be prepared by sol-gel process. This method is based on hydrolysis and condensation reaction of molecular precursors such as metal alkoxides and inorganic salts [11]. Sol-gel is a widely used technique for production of titanium dioxide nanopowders. It is a low cost and easy processing method for the preparation of titania powder. This method is based on hydrolysis and condensation reaction of molecular precursors such as metal alkoxides and inorganic salts. Metal alkoxides which are used as precursor material for sol-gel process are generally highly reactive species. Among transition-metal oxide materials, nanostructure titanium dioxide has been intensively investigated as a select platform on which an exceptionally wide range of appealing solid-state physico-chemical properties co-exist with the potential for low cost and

\*Corresponding author: **Ramesh P.S**  
Physics Wing DDE

environmental remediation and energy technologies. For improving crystallinity, post-calcination is generally required. High-temperature treatment results in size-increment and agglomeration [12].

In this paper, highly-crystalline anatase and rutile nanoparticles synthesized by the newly developed sol-gel method is illustrated. Effect of aging treatments on nanoparticles size and crystal structure is investigated. Products are characterized by XRD, FT-IR, Scanning electron microscopy (SEM), UV-Vis spectroscopy and photoluminescence (PL).

## Experimental

## MATERIALS

All chemicals were in analytical grade and were used as received without any additional purification. Titanium tetra isopropoxide [ $\text{Ti}(\text{OPri})_4$ ], (97%, Alpha) was used as starting precursor for synthesizing crystalline  $\text{TiO}_2$  particles. Hydrochloric acid (HCl) (37%, Merck) was used as a catalyst for alkoxide hydrolysis. Deionized water was used for the hydrolysis of  $\text{Ti}(\text{OPri})_4$ .

## Synthesis

The  $\text{TiO}_2$  colloidal solution was prepared by hydrolysis of titanium tetra isopropoxide (TTIP). In a typical process, 1M of titanium tetra isopropoxide was mixed together with 4 M of Hydrochloric acid (HCl). The resultant solution is mixed with 10M of distilled water and the solution was stirred vigorously for 8h to obtain a clear solution. The solution was then aged at room temperature for 24 h; the sols were transformed into gels, and washed with ethanol. After an aging period the solution was kept in an oven and dried at ( $130^\circ\text{C}$ ) and held at that temperature for four different constant hours (12,24,36 and 48 h). Also these products were thermally treated at 500, 600 and  $700^\circ\text{C}$  for 5h. After the beaker was cooled to ambient temperature, the resulting precipitates were washed with nitric acid and dried at room temperature for 1 hour. It was then crushed into fine powders with mortar.

## Characterizations

The X-ray diffraction patterns of the samples were recorded on a XPERT-PRO X-ray diffractometer with Cu-K radiation of wavelength  $1.5406 \text{ \AA}$  in  $2\theta$  range from  $20^\circ$  to  $70^\circ$ . UV-Visible spectrophotometer was using shimadzu UV-1650. Fourier transform infrared (FT-IR) spectroscopy measurement was recorded with AVATAR 330 FT-IR spectrometer in the range of  $4000\text{-}400 \text{ cm}^{-1}$ . The photoluminescence (PL) spectra of the sample were recorded by using VARIAN photoluminescence. SEM image was taken using JEOL, Model JSM 6390.

## RESULTS AND DISCUSSION

### X-ray diffraction studies

Fig.1 shows XRD patterns of the products obtained after aging at  $130^\circ\text{C}$  for different durations. These patterns illustrate pure anatase crystalline structure in all  $\text{TiO}_2$  nanopowders aged at

$130^\circ\text{C}$ . Comparison of four XRD patterns for  $130^\circ\text{C}$  shows that the diffraction peaks sharpened with increasing calcination time (48 hours), indicating increasing crystallite size. The average crystal size of the samples were calculated using the scherrer equation,  $D=K / \cos$ . The obtained grain sizes are 31 nm (12h), 39 nm (24 h), 45(36h) and 50 nm (48 h) for sample prepared at  $130^\circ\text{C}$  respectively. The result showed that the crystal size increased with increasing calcination time. An average crystal size of around 41 nm for  $130^\circ\text{C}$  was obtained for nanotitanium dioxide samples. The nanocrystalline anatase structure was confirmed by (101), (004), (200), (105), (204) and (116) diffraction peaks [13].

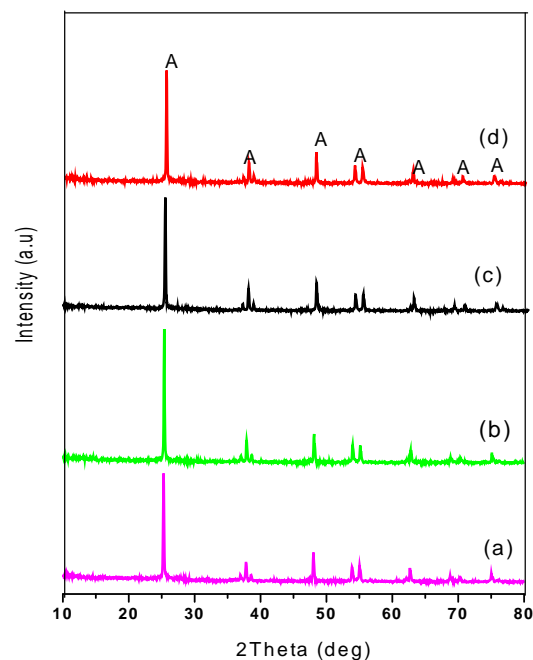


Figure 1 X-ray diffraction spectrum of nano titanium dioxide at  $130^\circ\text{C}$ , (a) 12h, b (24), (c) 36h, (d) 48h

Fig. 2 shows the XRD patterns of  $\text{TiO}_2$  nanoparticles (a) calcined at  $500^\circ\text{C}$ , (b)  $600^\circ\text{C}$ , and (c)  $700^\circ\text{C}$  for 5 h. It can be obviously seen from the XRD that partial crystallization appears just after drying and the phase structure of the powder calcined at temperatures below  $600^\circ\text{C}$  is mainly anatase type. The phase transformation from anatase to rutile occurred at about  $600^\circ\text{C}$ . At  $700^\circ\text{C}$  both anatase and rutile phase was observed. The observed anatase peaks at  $2\theta$  of 25.2, 37.8, 48.02, 53.9, 55.0, 62.7 and  $68.7^\circ$  represent the diffraction of the (101), (004), (200), (105), (211), (204) and (116) crystal planes respectively. (JCPDS 21-1272). As the temperature increased at  $700^\circ\text{C}$  the observed rutile peaks at  $2\theta$  of 27.45, 36.09, 41.23, 54.32 and  $56.64^\circ$  represent the diffraction of the (110), (101), (111), (211) and (220) crystal planes respectively. (JCPDS 01-075-1750). The crystal size of the prepared  $\text{TiO}_2$  calcined at 500, 600 and  $700^\circ\text{C}$  were estimated to be 29.2, 35.3 and 42.24 nm by the scherrer's equation, respectively. Obviously, the grain size increases with the increasing calcinations temperature. With increasing of calcination temperature the intensities of the peaks increased.

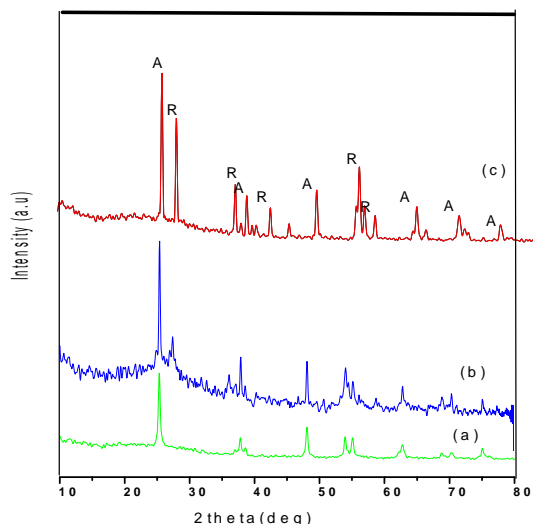


Figure 2 X-ray diffraction spectrum of nano titanium dioxide at (a) 500°C, (b) 600°C and (c) 700°C

### Effect of calcination time and temperature

The aging time and temperature is one of the preparation parameter that can influence the formation of nano titanium dioxide. In order to study this influence, nano titanium dioxide catalysis were prepared by changing the aging time from 12 to 48 h. At low calcination temperatures the prolongation of calcination time has little influence upon the particle size. The result showed that the crystal size increased with increasing calcinations time. In order to evaluate the effect of calcination temperature on crystallite size and phase content of TiO<sub>2</sub> nanoparticles. As can be seen in the XRD spectra with increasing calcination temperature, anatase phase percent decreases while rutile phase percent increases. Increasing calcination temperature increases the crystallite size of TiO<sub>2</sub> nanoparticles.

### Functional group Analysis (FT-IR)

The FT-IR spectra of the titanium dioxide at 130°C were represented in Fig. 3. The absorption band at 1630 cm<sup>-1</sup> is attributed to the stretching mode of the OH group and the bending mode of molecular water respectively. The broad band over the range of 400-700cm<sup>-1</sup>, related to bending and stretching mode of Ti-O-Ti and characteristic of well-ordered TiO<sub>6</sub> octahedrons. Ti-O and O-Ti-O- flexion vibration give rise to the broad absorption bands at 400 cm<sup>-1</sup> and 800 cm<sup>-1</sup> [14]. There is no peak 2910cm<sup>-1</sup> regarding to C-H stretching band, which means all organic compounds removed from the samples. The peaks at about 1394 cm<sup>-1</sup> correspond to the scissoring vibration of -CH<sub>3</sub> [15].

The infrared spectroscopy of TiO<sub>2</sub> at 500, 600 and 700° C were represented in Fig. 4. The absorption band at 1626.3 cm<sup>-1</sup> is attributed to the stretching mode of O-H bonds in absorption water. The peak at 1620 cm<sup>-1</sup> was caused by bending vibration of coordinated H<sub>2</sub>O as well as from the Ti-OH, and this band could be normally reduced by the calcination process at higher temperature [16], showing that a certain amount of O-H groups in TiO<sub>2</sub> were removed during the calcinations. The bands

between 3600 and 3000 cm<sup>-1</sup> are due to hydroxyl stretching and NH- stretching vibration bands. The absorption band at 3435 cm<sup>-1</sup> is due to coupling of hydroxyl (OH) stretching and NH-stretching vibrations. The hydroxyl groups can the photo-induced holes (h<sup>+</sup>) when irradiated with light and then form hydroxyl radicals (·OH) with high oxidation capability. The peak observed in the range of 2356–2364 cm<sup>-1</sup> was due to amine (NH) group stretching frequency [17].

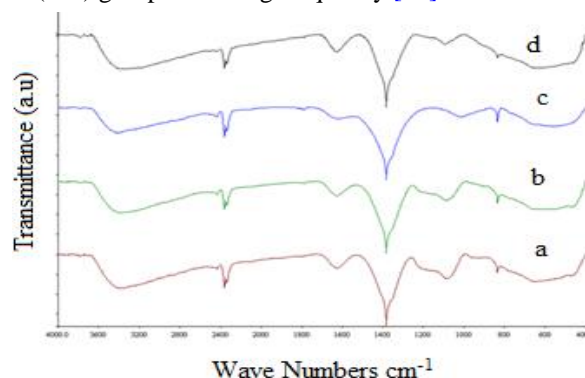


Figure 3 FT – IR spectra of nano Titanium dioxide at 130°C, (a) 12h, b (24), (c) 36h, (d) 48h

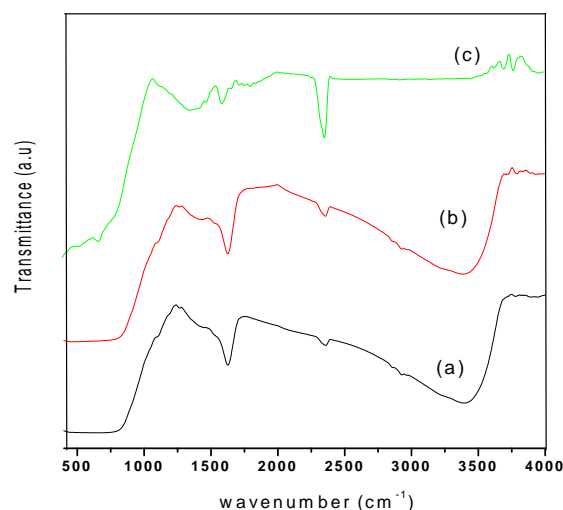


Figure 4 FT – IR spectra of nano Titanium dioxide at (a) 600°C, (b) 600° C and (c) 700°C

### Surface Morphological Analysis (SEM)

The surface morphology of the nano titanium dioxide was obtained from scanning electron microscopy (SEM).

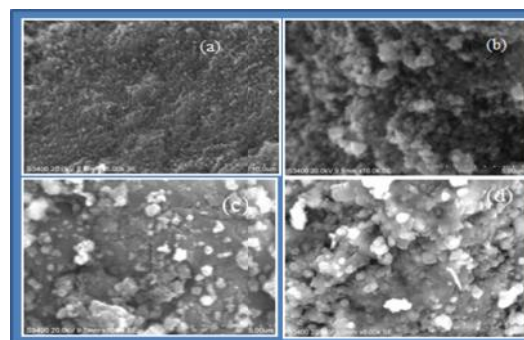


Fig.5 SEM photographs of titanium dioxide at 130°C (a) 12h, (b) 24 h, (c) 36h and (d) 48 h

Fig. 5. shows the SEM picture of nano titanium oxide calcined at 130°C for four different calcination time (12, 24, 36 and 48 h). It is observed that nano titanium dioxide particles are spherical in shape. The particles of the material all have spherical or spheroidal morphology. At higher temperature spherical shape with slight agglomerated together.

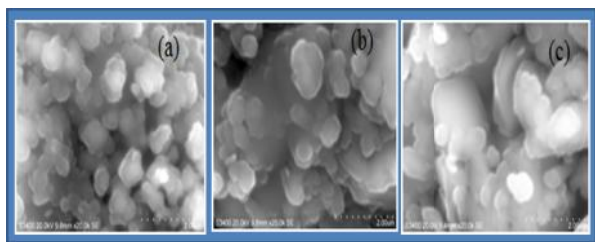


Figure 6 SEM photographs of titanium dioxide at (a) 500, (b) 600 and (c) 700° C

As shown from Fig. 6. The calcination temperature increases the size of the nanoparticles is also increases. This figure shows high homogeneity emerged in sample by increasing the calcination temperature. Whatever the calcination temperature was low, the samples were less agglomerated. With increasing the calcination temperature boundaries between nanoparticles were better and the morphology of particles changed to spherical shape and the nanopowder were more agglomerated.

#### Photoluminescence studies (PL)

The photoluminescence (PL) emission spectra are commonly used to reveal the efficiency of the trapping, transfer and separation of charger carriers, within an activated semiconductor photocatalyst [18]. The transfer behavior of the electron-hole pairs in the TiO<sub>2</sub> samples can be studied by the recombination of the free charges, which contributes significantly to emission signals of the PL spectra [19]. The PL spectra of three samples were examined in the range of 320–550 nm in our study, as shown in Fig. 7. TiO<sub>2</sub> nanoparticles could exhibit an obvious PL peaks at about 450 nm with the excited wavelength of 300 nm possibly resulting from binding exactions [20]. There were lots of oxygen vacancies on the surface of TiO<sub>2</sub> nanoparticles, and the size of particle was fine so that the average distance the electrons could move freely was very short. These factors could make the oxygen vacancies very easily bind electrons to form excitons. Thus, the exciton energy level near the bottom of the conduction band could come into being and the PL band of the excitons showed could also occur.

The UV emission is arising due to phonon assisted indirect transition, 438 nm is due to self-trapped exciton localized on TiO<sub>6</sub> octahedral. The peaks at 463 nm and 537 nm is due to the oxygen vacancies, and the other at 468 nm was related to surface trap state owing to incomplete surface passivation, where radiation less recombination occurred. Since PL emission was the result of the recombination of excited electrons and holes, the lower PL intensity of the modified sample indicated a lower recombination rate of excited electrons and holes [21].

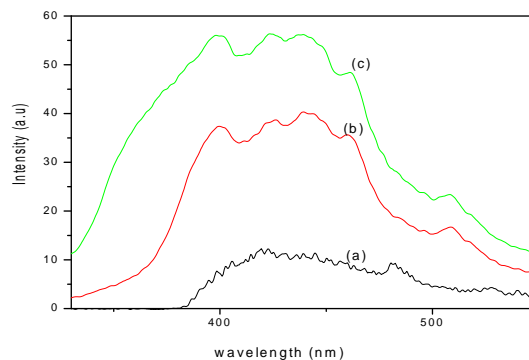


Figure 7 PL spectra of titanium dioxide at (a) 500, (b) 600 and (c) 700° C

#### UV-Vis spectroscopy

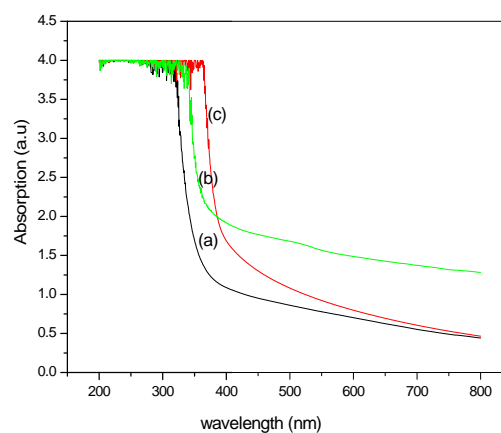


Figure 8 UV-Vis spectra of pure TiO<sub>2</sub> (a) 500, (b) 600 and (c) 700° C

The UV-Vis spectra of pure TiO<sub>2</sub> at 500, 600 and 700° C are given in Fig. 8. The band gap adsorption edge is approximately 380 nm, which does not exhibit noticeable adsorption in the visible regime. With increasing temperature, these samples present an enhancement of the light adsorption in the visible range. All the TiO<sub>2</sub> samples, however, exhibit a red shift of the absorption edge.

#### CONCLUSION

Nano TiO<sub>2</sub> powders have been prepared by sol-gel method successfully. The results obtained from XRD showed the pure anatase TiO<sub>2</sub> was found at 130°C. Different calcination time was found to produce different effects upon the grain size depending upon calcination temperature. The phase structure of the powder calcined temperature below 600° C is mainly of anatase type. The phase transformation from anatase to rutile occurred at about 600° C and both anatase and rutile phases observed at 700°C. Obviously, the grain size increases with the increasing calcination temperatures. With increasing of calcination temperature the intensities of the peaks increased. At higher temperature the spherical shape with slight agglomerated together. The different peaks in PL spectra could be owing to the recombination of photoinduced electrons and holes, free or trapped excitons emission and the surface states and presence of anatase and rutile phases of TiO<sub>2</sub>. TiO<sub>2</sub>

nanoparticles could exhibit an obvious PL peaks at about 450 nm with the excited wavelength of 300 nm possibly resulting from binding exactions. These properties result in excellent photocatalytic activity to degrade organic substances and good sedimentation to recover titanium dioxide.

## References

1. Pal, K., T. P. Majumder, C. Neogy, and Debnath, S. C. 2012. Optical, dielectric and microscopic observation of different phases TiO<sub>2</sub> metal host nanowires. *Journal of Molecular Structure*. 1016:30–38.
2. Chaure, N. B., A. K. Ray, and Capan, R. 2005. Sol-gel derived nanocrystalline titania thin films on silicon. *Semiconductor Sci. Technol.* 20: 788–792.
3. Li-Piin Sung, Stephanie Scierka, ManaBaghai-Anaraki and Derek L, Ho. 2003. Characterization of Metal-Oxide Nanoparticles: Synthesis and Dispersion in Polymeric Coatings Mater. Res Soc Symp Proc. 740: 115.4.
4. Xu, J. X., L. P. Li, Y. J. Yan, H. Wang, X. X. Wang, X. Z., and Li, G. S. 2008. Synthesis and photoluminescence of well-dispersible anatase TiO<sub>2</sub> nanoparticles. *Journal of Colloid and Interface Science*. 318: 29–34.
5. Wn, Y., and Yang, P. 2001. Direct Observation of Vapor-Liquid-Solid Nanowire Growth. *J. Amer. Chem. Soc.* 123:3165-3166.
6. Pradhan, S.K., P.J. Reucrofr, F. Yang, and Dozier, A. 2003. Growth of TiO<sub>2</sub> nanorods by metalorganic chemical vapor deposition. *J. Crystal Growth* 256: 83-88.
7. Morales, A.M., and Lieber, C.M. 1998. A laser ablation method for the synthesis of crystalline semiconductor nanowires. *Science* 279: 208-211.
8. Sugimoto, T., X. Zhou, and Muramatsu, A. 2003. Synthesis of uniform anatase TiO<sub>2</sub> nanoparticles by gel-sol method. *J. Colloid and Interface Science* 259: 53-61.
9. Chung – sikkim, Byungkee Moon, Jong – Ho park, Byung – chunchoi, and Hyo – Jinseo 2003. Solvothermal synthesis of nanocrystalline TiO<sub>2</sub> in toluene with surfactant. *Journal of crystal growth* 257: 309-315.
10. Lakshmi, B.B., P.K. Dorhout, and Martin, C.R. 1997. Sol-gel template synthesis of semiconductor nanostructure. *Chem. Mater.* 9: 857-862.
11. Livage, J., M. Henry, C. Sanchez, 1988. Sol-gel chemistry of Transition Metal oxides. *Progress in solid state chemistry* 18:259-341.
12. Tang, Z., J. Zhang, Cheng Z and Zhang Z. 2002. Synthesis of nanosized rutile TiO<sub>2</sub> powder at low temperature. *Mater. Chem. Phys.* 77:314-317.
13. Venkatachalam, N., M. Palanichamy, V. Murugesan 2007. Sol-gel preparation and characterization of nanosize TiO<sub>2</sub>: Its photocatalytic performance
14. *Materials chemistry and physics* 104: 454-459.
15. Samira Bagheri, Donya Ramimoghadam, Amin Termeh Yousefi, and Sharifah Bee Abd Hamid. 2015. Synthesis, Characterization and Electrocatalytic Activity of Silver Doped-Titanium Dioxide Nanoparticles. *Int. J. Electrochem. Sci.* 10: 3088 – 3097.
16. Yang, J., H.Z. Bai, X.C. Tan, Lian, J.S. 2006. IR and XPS investigation of visible-light photocatalysis-Nitrogen-carbon-doped TiO<sub>2</sub> film. *Appl. Surf. Sci.* 253 1988–1994.
17. Chen, Y.F., C.Y. Lee, M.Y. Yeng, and Chiu, H.T. 2003. The Effect of Calcination Temperature on the Crystallinity of TiO<sub>2</sub> Nanopowder. *J. Cryst. Growth*. 247: 363-370.
18. Devanand Venkatasubbu, G., S. Ramasamy, and V. Ramakrishnan, Kumar, J. 2013. Folate targeted PEGylated titanium dioxide nanoparticles as a nanocarrier for targeted paclitaxel drug delivery. *Advanced Powder Technology*. 24:947-954.
19. Liu, J., R. Han, H. Wang, Y. Zhao, Z. Chu, and Wu, H. 2011. Photoassisted degradation of pentachlorophenol in a simulated soil washing system containing nonionic surfactant Triton X-100 with La-B codoped TiO<sub>2</sub> under visible and solar light irradiation. *Appl. Catal. B: Environ.* 103:470–478.
20. Shen, X., B. Tian, and Zhang, J. 2013. Tailored preparation of titania with controllable phases of anatase and brookite by an alkaline hydrothermal route. *Catal. Today* 201:151–158.
21. Li, D., Y. Zhen, X. Fu, *Chin. J.* 2000. *Mater. Res.* 14:639.
22. Xu, J. X., L. P. Li, Y. J. Yan, H. Wang, X. X. Wang, X. Z., and G. S. Li. 2008. Synthesis and photoluminescence of well-dispersible anatase TiO<sub>2</sub> nanoparticles. *Journal of Colloid and Interface Science*. 318: 29–34.

\*\*\*\*\*

### How to cite this article:

Kavitha V, Ramesh P.S and Geetha D. 2015, Synthesis and Characterization of Nano Titanium Dioxide Via Sol Gel Process At Different Calcination Time And Temperature. *Int J Rec Sci Res* Vol. 6, Issue, 12, pp. 7909-7913.

ISSN 0976-3031



9 770976 303009 >